Journal of Inclusion Phenomena and Molecular Recognition in Chemistry **20:** 381–391, 1995.

Formation of a Disordered Layer Lattice during the Intercalation of Water into Anhydrous Vanadyl Phosphate

LUDVÍK BENEŠ and VÍTĚZSLAV ZIMA
Joint Laboratory of Solid State Chemistry of the Academy of Sciences of the Czech Republic and University of Pardubice, Studentská 84, 530 09 Pardubice, Czech Republic.

(Received: 20 October 1994; in final form: 30 January 1995)

Abstract. The course of intercalation of water into α_1-$VOPO_4$ has been studied by thermomechanical analysis and X-ray diffraction. Neither formation of vanadyl phosphate monohydrate nor staging were observed during the intercalation. The broadening and the shift of the positions of the lines in the diffractograms have been explained by the random stacking of intercalated and nonintercalated layers in the sample.

Key words: Intercalation, X-ray powder diffraction, vanadyl phosphate.

1. Introduction

Intercalation of various atoms, molecules or ions into layered solids leads to new materials often with interesting properties. Studies of the kinetics and mechanism of the intercalation processes, in which the guest species are atoms, have been reviewed in [1]. Several possible phenomena during these intercalations have been observed and described:

(i) in the crystal of the host intercalated and nonintercalated parts of the crystal coexist; a two phase system is formed, with a transition area, which has been designed as an advancing phase boundary [2, 3];
(ii) due to interactions across the layers a superstructure is generated in the crystal [4]. When these interactions lead to a regular alternation of empty interlayer spaces (galleries) and galleries filled with guest, so-called staging is observed [5]. The filled galleries are not usually spread over the whole crystal, but the guest creates islands known as Daumas–Hérold zones [6].
(iii) in cases where the empty and full galleries alternate randomly, the so-called Hendricks–Teller effect occurs [7].

On the other hand, little is known about the kinetics and mechanism of intercalation of molecules. The monitoring of intercalation by real-time *in situ* X-ray diffraction [8] and the kinetic measurements of intercalation of liquid molecular guests into

layered hosts based on the change of the total volume of the reaction system [9] have been described. The mechanism of intercalation has been suggested [10], in which the ability of the host to intercalate molecules is correlated with the calculated flexibility of the host layers.

Layered vanadyl phosphate is able to intercalate both neutral molecules and cations. Vanadyl phosphate dihydrate reacts with cations in the presence of a reducing agent changing the oxidation state of V(V) to V(IV) simultaneously [11]. Staging was observed in this host during intercalation of lithium and sodium ions [12, 13]. Alcohols [14], amines [15, 16], carboxylic acids [17] and pyridine [18] can intercalate in the interlayer space of anhydrous vanadyl phosphate. From this point of view, vanadyl phosphate dihydrate can be regarded as an intercalate of $VOPO_4$ with water.

The structure of $VOPO_4 \cdot 2H_2O$ has been determined by X-ray diffraction [19] and neutron diffraction [20]. Layers of vanadyl phosphate are formed from corner sharing vanadium octahedra and phosphate tetrahedra. Vanadium octahedra are composed from four equatorial oxygens which are shared by phosphorus. One of the axial oxygens is a vanadyl oxygen, and the second one belongs to a water molecule coordinated to vanadium. The second water molecule is bonded by a weak H-bridge between layers. The structure is tetragonal with a = 6.215, c = 7.403 Å and space group $P4/n$. Several modifications of anhydrous vanadyl phosphate are known [21, 22]. The most important of them is α_1-$VOPO_4$ (c=4.2 Å), which is formed by dehydration of $VOPO_4 \cdot 2H_2O$.

The interlayer water is released in two steps during heating of $VOPO_4 \cdot 2H_2O$. The first molecule of water is liberated at 44 °C producing the monohydrate with c=6.3 Å as observed by XRD and thermomechanical analysis [23]. The second dehydration step occurs at 80 °C. The temperatures of dehydration obtained from DTA are slightly higher [24].

The aim of this work was to contribute to elucidation of the mechanism of intercalation of water in α_1-$VOPO_4$ by X-ray diffraction and thermomechanical analysis.

2. X-Ray Diffraction of a Hendricks–Teller Disordered Layered Lattice

Layered crystals are not completely ordered in some cases. One type of disorder may be defined as a random irregular sequence of layers of different kinds. This irregularity leads to variation of diffraction angles and linewidths in the X-ray diffraction pattern [7, 25]. The Hendricks–Teller theory can be used for the description of this phenomenon if the following conditions are assumed: (i) only two types of layers are present with interlayer distances d_1 and d_2; (ii) both layers have the same structure factor; (iii) fractions f_1 and f_2 correspond to interlayer distances d_1 and d_2, respectively; (iv) the dimensions of the crystallite are macroscopic [26]; (v) geometric factors in the X-ray experiment are not considered, (vi) thermal factors

are neglected. Under these assumptions, the scattered intensity for a Bragg angle may be described by the formula [25]:

$$I_{av} = |V_L|^2 \frac{1 - C^2}{1 - 2C\cos\bar{\Phi}} \tag{1}$$

where I_{av} is the average scattered intensity per layer, V_L is the layer form factor, and

$$C = f_1 \cos(\Phi_1 - \bar{\Phi}) + f_2 \cos(\Phi_2 - \bar{\Phi}) \tag{2}$$

where

$$\bar{\Phi} = \arctan \frac{f_1 \sin\Phi_1 + f_2 \sin\Phi_2}{f_1 \cos\Phi_1 + f_2 \cos\Phi_2} \tag{3}$$

and

$$\Phi_i = (4\pi d_i/\lambda)\sin\Theta \tag{4}$$

where $i = 1$ or 2, respectively, and d_i is interlayer distance. A slight dependence of the layer form factor V_L on the diffraction angle Θ does not affect the computed basal plane linewidths and positions. The main term determining the positions, line shapes, and widths is $I_{av}/|V_L|^2$ in Equation (1). Three independent variables d_1, d_2, and f_1 are contained in this equation. The linewidths computed by this method correspond to disorder of layers only, while the measured linewidths are influenced among other factors by the instrument linewidth.

3. Experimental

Vanadyl phosphate dihydrate was prepared by prolonged boiling of a mixture of vanadium pentoxide and phosphoric acid in water [24]. The polycrystalline product was separated by sieve analysis and the fraction with the particle size 0.1 to 0.2 mm was used for XRD. For the thermomechanical analysis, $VOPO_4 \cdot 2H_2O$ was recrystallized from the mother solution by standing for 30 days at room temperature [23]. In this way squared flat crystals with dimensions of 1 × 1 mm and thickness about 0.05 mm were obtained.

Powder data were obtained with an HZG-4 X-ray diffractometer (Freiberger Präzisionsmechanik, Germany) using CuK_α radiation with discrimination of the CuK_β radiation by a nickel filter. Diffraction angles were measured from 5 to 30° (2Θ). Every cycle of measurement lasted 8 minutes. The CuK_{α_2} intensities were removed from the original data. The positions and linewidths of the diffraction lines were determined by a Lorentz function fitting. The measurements were carried out on a heated corundum plate with a thermocouple. The powder sample was placed on the plate, heated to 250 °C, and kept at this temperature for about 1 hour to

obtain dehydrated α_1-$VOPO_4$. The sample was then cooled to 25 °C by flowing dry air (flow rate 0.5 L min^{-1}). The time measurements were carried out in a flow of wet air (air was bubbled through water at 22 °C and at the same flow rate). The sample temperature was kept 3 °C higher than the flowed air temperature to avoid moistening of the sample.

The thermomechanical measurement was carried out with a TMA CX03R dilatometer described previously [27] with a differential capacitance probe detector. The detector is controlled by a unique electronic system that ensures excellent baseline stability and resolution of about 10^{-8} m. The parent monocrystal of $VOPO_4 \cdot 2H_2O$ was heated to 200 °C to prepare dehydrated α_1-$VOPO_4$ and then quickly cooled to room temperature. The time dependence of changes of thickness of the crystal was then followed at this temperature. The sample was in a flow of wet air with 45% relative humidity. In the second experiment, the dehydration of $VOPO_4 \cdot 2H_2O$ to monohydrate and back hydration to dihydrate was followed with a heating and cooling rate of 0.2 K min^{-1} without air flowing. The force applied to the sample was 50 mN in both experiments.

4. Results and Discussion

The changes of thickness of the crystal of $VOPO_4 \cdot 2H_2O$ during heating are shown in the left part of Figure 1. The original thickness of the dihydrate (l = 0.059 mm) decreases relatively rapidly to 0.047 mm (monohydrate) and then more slowly to 0.027 mm (dehydrated α_1-$VOPO_4$). This two step dehydration is in agreement with Ref. [23]. The right part of Figure 1 describes the behavior of the dehydrated sample left at room temperature in the flow of wet air, i.e. intercalation of water into α_1-$VOPO_4$. The thickness of the crystal returns to the original value in 1.5 h. The dependence of the thickness on time has an exponential shape. No significant dwell corresponding to a monohydrate formation is observed in this part of the figure. Staging, which was described in systems of carbon–H_2SO_4 and TaS_2–K [28], was not observed in our case.

Thermomechanical analysis of the $VOPO_4 \cdot 2H_2O$ sample during heating to 70 °C (curve 1) and cooling to 30 °C (curve 2) is shown in Figure 2. Liberated water is probably adsorbed at the surface of the crystal in this temperature region. Therefore intercalation of water into $VOPO_4 \cdot H_2O$ during cooling does not need flowing of wet air and passes very quickly. At the cooling rate of 1 K min^{-1} this process is finished in 5 min.

Changes of the diffractograms during intercalation of water into α_1-$VOPO_4$ and interlayer distances of all lines for all patterns are given in Figures 3 and 4, respectively. As seen from both figures, the original α_1-$VOPO_4$ (basal spacing 4.2 Å) is changed to $VOPO_4 \cdot 2H_2O$ (basal spacing 7.4 Å). Lines of vanadyl phosphate monohydrate, which has a very intensive (001) line (d = 6.3 Å[23]), were not observed during hydration. Diffractograms do not show sets of (00ℓ) lines corresponding to staging of the sample. The positions of lines of the (00ℓ) type

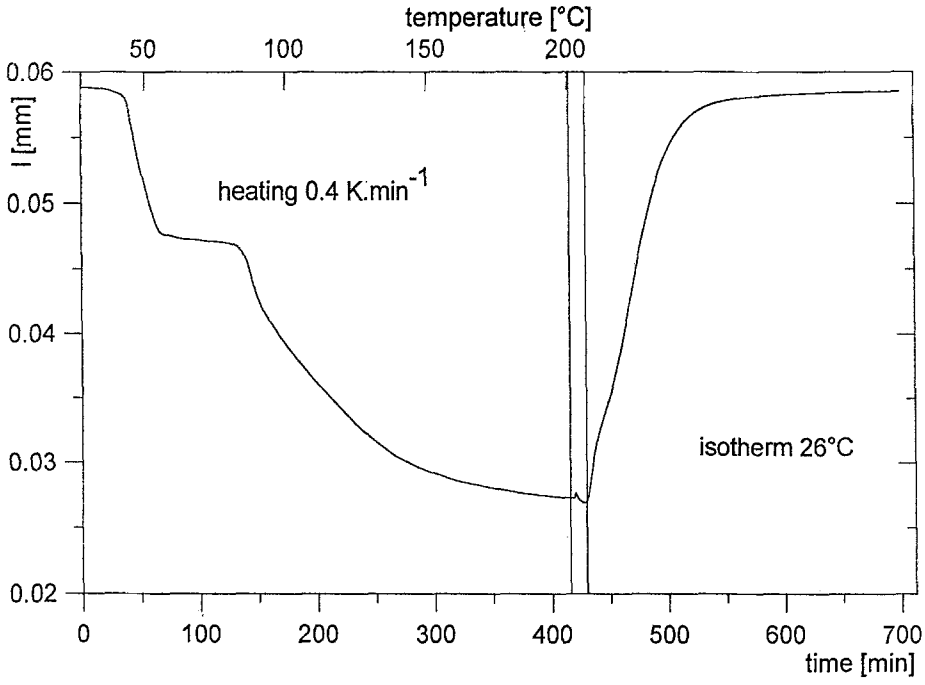

Fig. 1. The changes of the thickness l of the crystal of $VOPO_4 \cdot 2H_2O$ during heating, cooling, and during intercalation of water at 26 °C.

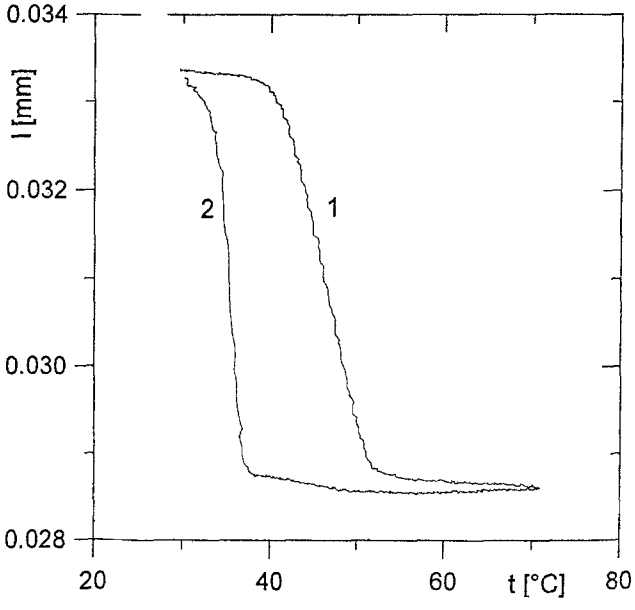

Fig. 2. Thermomechanical analysis of the sample during heating (1) and cooling (2).

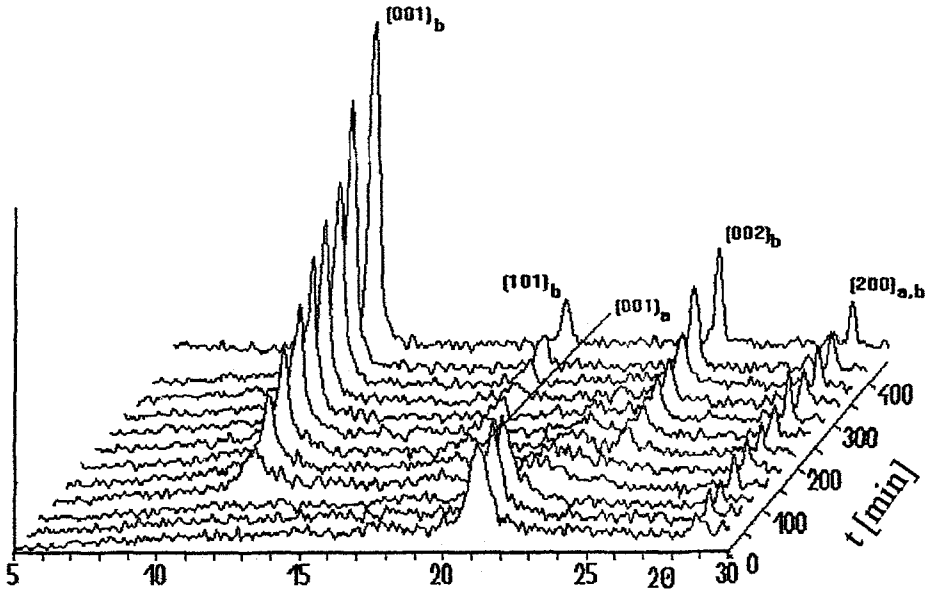

Fig. 3. The changes of the diffractograms during intercalation of water into α_1-$VOPO_4$ (index 'a' stands for anhydrous vanadyl phosphate, index 'b' for $VOPO_4 \cdot 2H_2O$).

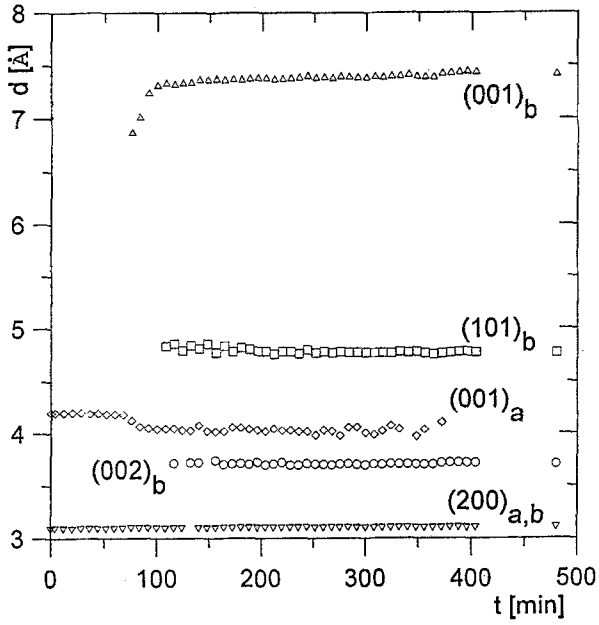

Fig. 4. Dependence of the interplanar distances d on the time t of the intercalation of water into α_1-$VOPO_4$.

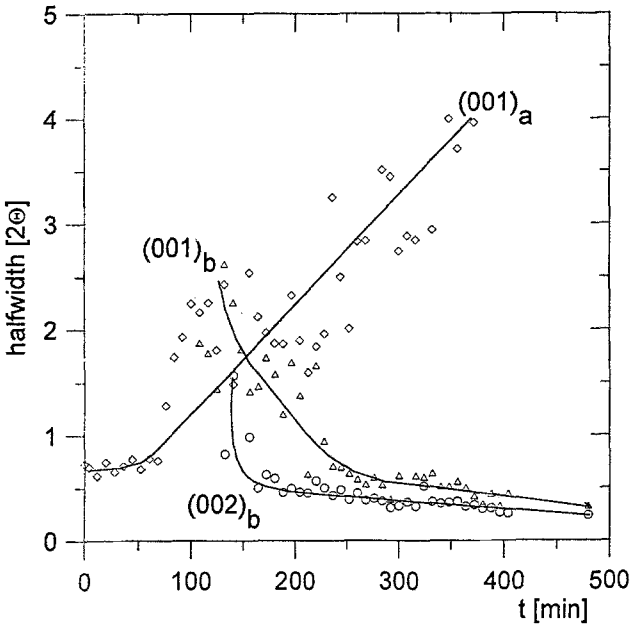

Fig. 5. Dependence of the halfwidths on the time t of the intercalation of water into α_1-$VOPO_4$.

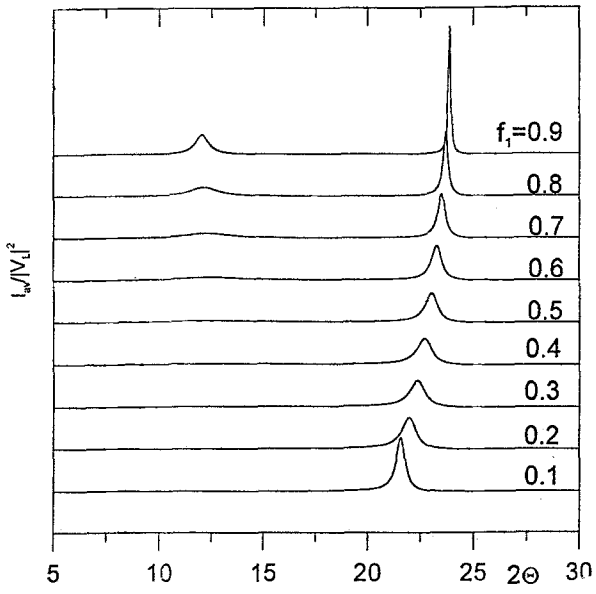

Fig. 6. Changes of the Hendricks–Teller function (see Equations 1–4) as a function of the fraction f_1 (the amount of $VOPO_4 \cdot 2H_2O$ layers in the sample).

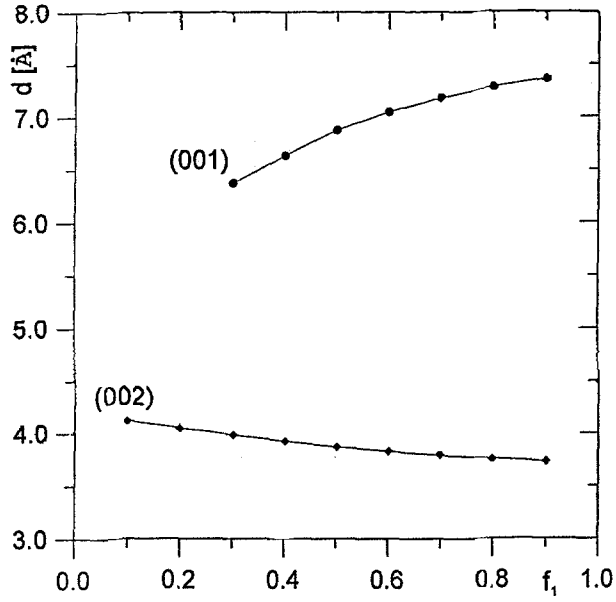

Fig. 7. Dependence of the interplanar distances d calculated from the Hendricks–Teller function on the fraction f_1.

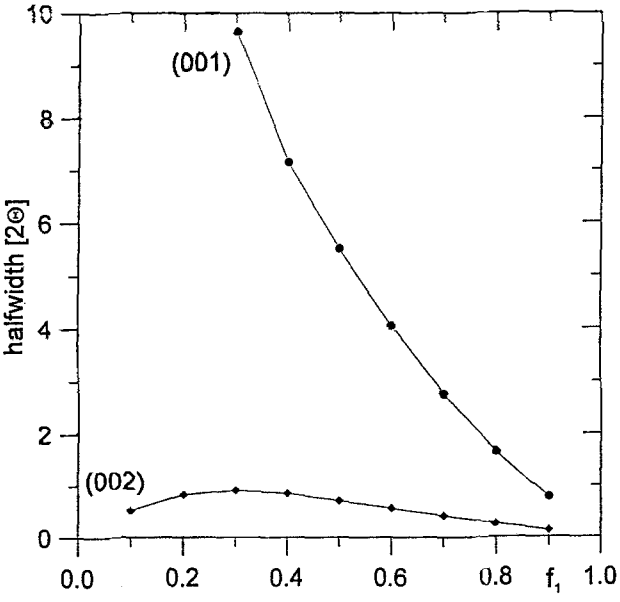

Fig. 8. Dependence of halfwidths calculated from the Hendricks–Teller function on the fraction f_1.

do not correspond sufficiently exactly to interlayer distances of pure phases of α_1-$VOPO_4$ or $VOPO_4 \cdot 2H_2O$, in contrast to Ref. [8], in which only the diffraction

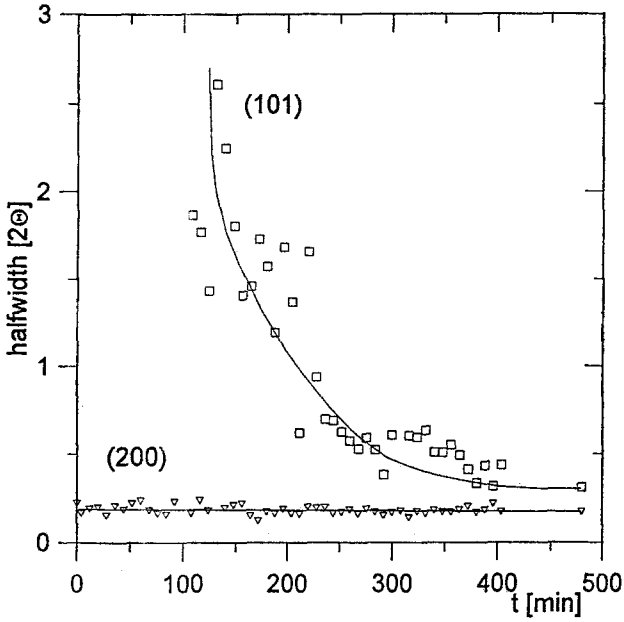

Fig. 9. Dependence of observed halfwidths on the time t of intercalation of water into α_1-$VOPO_4$.

lines of the parent host and the intercalate formed were observed. The interplanar distance belonging to the (001) line of anhydrous vanadyl phosphate gradually decreases (marked 'a' in Figure 4), and the linewidth of this line (see Figure 5) increases at the same time. Similarly, the (001) and (002) interplanar distances of $VOPO_4 \cdot 2H_2O$ (marked 'b' in Figure 4), which appears during hydration, are at first significantly shifted and become gradually closer to values corresponding to pure $VOPO_4 \cdot 2H_2O$. At first, these lines are remarkably broad. The linewidths of these lines decrease to a value of 0.25° (2Θ) as seen in Figure 5.

The broadening of the (00ℓ) lines of both phases (α_1-$VOPO_4$, $VOPO_4 \cdot 2H_2O$) can be explained by fragmentation of the microcrystals during the intercalation of water, but the shifts of the line positions remain unexplained. The above behavior can be elucidated by formation of a Hendricks–Teller disordered layered lattice. Let us assume that the layers of $VOPO_4 \cdot 2H_2O$ appear among the layers of α_1-$VOPO_4$ randomly in the crystal during the intercalation of water. Intercalation of the second molecule of water follows intercalation of the first molecule immediately, so it is possible to neglect the amount of monohydrate layers. Thus, we have d_1 = 7.4 Å (basal spacing of $VOPO_4 \cdot 2H_2O$) and d_2 = 4.2 Å (basal spacing of α_1-$VOPO_4$) for the Hendricks–Teller function $I_{av}/|V_L|^2$ in Equations 1–4. The dependences of the Hendricks–Teller function on the diffraction angle 2Θ for various ratio of fractions f_1 and f_2 are given in Figure 6. The dependences of the interplanar distances and linewidths of the (001) and (002) lines on the fraction f_1 calculated by the Hendricks–Teller functions are shown in Figures 7 and 8, respectively. As

is obvious from both figures, the positions and linewidths of the (001) line are more influenced by the phase with random alternation of layers of α_1-$VOPO_4$ and $VOPO_4 \cdot 2H_2O$ than the positions and linewidths of the (002) line. It is caused by the fact that the value of the basal spacing of α_1-$VOPO_4$ is close to half the value for $VOPO_4 \cdot 2H_2O$.

The Hendricks–Teller model describes the sample which is in a steady state, when all crystals contain the same amount of both randomly varying layers. The heterogeneous intercalation reaction takes place in the sample during our experiment. Thus it is possible to presume that in the sample crystallites with various content of intercalated water occur simultaneously, i.e. with various values of the fraction f_1. The observed diffractogram is then a superposition of diffractograms of all crystallites. The positions and linewidths of the diffraction lines of the individual crystallites are slightly different, so that the observed linewidths are greater than the calculated values from the Hendricks–Teller function. Besides this, the lines with smaller linewidths influence the line positions more in the observed diffractogram. It explains why a couple of the diffraction lines appears in the region of 21–24°2Θ which correspond to the fractions $f_1 < 0.2$ and $f_1 > 0.8$. The linewidth of the (001) line is very strongly influenced by the Hendricks–Teller function (Figures 6 and 8). As this line is very intense in $VOPO_4 \cdot 2H_2O$ (its integral intensity is five times greater than that of the (002) line), the diffractions of crystals with a higher degree of intercalation of water (i.e. with higher value of f_1) affect the observed diffractogram more distinctly. Therefore the interlayer distances increase very quickly to the value close to the basal spacing of $VOPO_4 \cdot 2H_2O$ during intercalation. The linewidth of this line diminishes at the same time. The (200) interplanar distances are not changed during intercalation of water into α_1-$VOPO_4$ (Figure 4). Also the linewidth of this line is almost constant (Figure 9). This is in agreement with the fact that the lattice parameter a of α_1-$VOPO_4$ and of vanadyl phosphate dihydrate is the same. It indicates also that the layers are not shifted in the direction of the a–a plane. On the other hand, the (101) diffraction of $VOPO_4 \cdot 2H_2O$, which appears during intercalation, has a large, gradually decreasing linewidth. This is explained by the existence of only small areas of the crystallites, in which the (101) planes may diffract at the beginning of the reaction. Therefore this line is distinctly broadened. The disorder of the intermediate regions of the crystallites may lead to broadening of this line due to the Hendricks–Teller effect. It would explain the fact that the interlayer distances are slightly shifted for this line.

5. Conclusions

Staging was not observed during intercalation of water into α_1-$VOPO_4$. In contrast to the deintercalation, the intercalation of water is not a two step process. The formation of vanadyl phosphate monohydrate was not proved. Molecules of water probably fill the interlayer space randomly, creating a Hendricks–Teller disordered layer lattice, which is composed from α_1-$VOPO_4$ and $VOPO_4 \cdot 2H_2O$ layers.

Acknowledgement

We thank the Grant Agency of the Czech Republic for financial support (grant no. 203/93/0157).

References

1. M.S. Whittingham and A.J. Jacobson (Eds.): *Intercalation Chemistry,* Academic Press, New York (1982).
2. A. Clearfield: *Chem. Rev.* **88**, 125 (1988).
3. G. Alberti: *Acc. Chem. Res.* **11**, 163 (1978).
4. G.A. Scholz, R.F. Frindt, and A.E. Curcon: *Physica Stat. Solidi (A)* **71** (1982).
5. M.S. Whittingham and M.B. Dines: *Surv. Prog. Chem.* **9**, 55 (1980).
6. N. Daumas and A. Hérold: *C. R. Seances, Acad. Sci., Ser. C* **268**, 373 (1969).
7. D.C. Johnston and S.P. Flysinger: *Phys. Rev. B* **30**, 980 (1984).
8. S.M. Clark, J.S.O. Evans, D. O'Hare, C.J. Nuttall, and H.V. Wong: *J.Chem.Soc., Chem. Commun.* 809 (1994).
9. J. Votinský, J. Kalousová, L. Beneš, I. Baudyšová, and V. Zima: *J. Incl. Phenom.* **15**, 71 (1993).
10. J. Votinský and L. Beneš: *Collect. Czech. Chem. Commun.* **56**, 2859 (1991).
11. A.J. Jacobson, J.W. Johnson, J.F. Brody, J.C. Scanlon, and J.T. Lewandowski: *Inorg. Chem.* **24**, 1782 (1985).
12. R. Šišková, L. Beneš, V. Zima, M. Vlček, J. Votinský, and J. Kalousová: *Polyhedron* **12**, 181 (1993).
13. V. Zima, L. Beneš, R. Šišková, P. Fatěna, and J. Votinský: *Solid State Ionics* **67**, 277 (1994).
14. L. Beneš, J. Votinský, J. Kalousová, and J. Klikorka: *Inorg. Chim. Acta* **114**, 47 (1986).
15. K. Beneke and G. Lagaly: *Inorg. Chem.* **22**, 1503 (1983).
16. L. Beneš, R. Hyklová, J. Kalousová, and J. Votinský: *Inorg. Chim. Acta* **177**, 71 (1990).
17. L. Beneš, J. Votinský, J. Kalousová, and K. Handlíř: *Inorg. Chim. Acta* **176**, 255 (1990).
18. J.W. Johnson, A.J. Jacobson, J.F. Brody, and S.M. Rich: *Inorg. Chem.* **21**, 3820 (1982).
19. H.R. Tietze: *Aust. J. Chem.* **34**, 2035 (1981).
20. M. Tachez, F. Theobald, J. Bernard, and A.W. Hewat: *Rev. Chim. Minerale* **19**, 291 (1982).
21. B. Jordan and C. Calvo: *Can. J. Chem.* **51**, 2621 (1973).
22. E. Bordes: *These d'Etat,* Compiegne (France), 1979.
23. V. Zima, L.Beneš, J. Málek, and M. Vlček: *Mat. Res. Bull.* **29**, 687 (1994).
24. G. Ladwig: *Z. Anorg. Allgem. Chem.* **338**, 266 (1965).
25. S. Hendricks and E. Teller: *J. Chem. Phys.* **10**, 147 (1942).
26. J. Mering: *Acta Crystallogr.* **2**, 371 (1949).
27. J. Málek and R. Švejka: *J. Non-Cryst. Solids* **172–174**, 635 (1994).
28. W. Biberacher, A. Lerf, J.O. Besenhard, H. Möhwald, and T. Butz: *Mat. Res. Bull.* **17**, 1385 (1982).